J Solid State Electrochem (2014) 18:13–18
DOI 10.1007/s10008-013-2224-y

ORIGINAL PAPER

Anodic electrodeposition of $Ag_{1-x}Cu_xO$ microcrystals

Anna M. Fyhn · Xiaodong Yang · Mohammadreza Nematollahi · John C. Walmsley · Ursula J. Gibson

Received: 24 June 2013 / Revised: 8 August 2013 / Accepted: 9 August 2013 / Published online: 28 August 2013

Abstract We demonstrate the anodic electrodeposition of copper-doped AgO at high pH using a silver counter-electrode. Precipitates from a mixture of nitrates and NaOH provided source material for the deposition, and application of a moderate anodic voltage (0.9 V) to the substrate led to deposition of crystalline nanoparticles with incorporated copper. Further increase of the NaOH concentration reduced the amount of copper in the crystals, and higher voltages degraded the crystal quality. XRD confirms the underlying structure to be that of AgO, and Auger and energy dispersive x-ray analyses confirm copper concentrations of approximately 3 % in the crystals.

Keywords Nanostructures · Oxides · Electrodeposition · Doping · Crystal morphology

Introduction

High pH electrodeposition, demonstrated by Switzer's group for copper oxide [1] which is of interest for solar cell applications, has opened up this technique as a low-cost scalable method for the formation of a wide variety of related materials. Cuprous oxide has been extensively studied [2–5] for solar cell applications, and has been deposited by both physical and chemical methods. Pure AgO and mixed copper and silver oxides have also attracted attention in this context. High pH deposition of Ag_2O [6], from diammenesilver(I) ions was recently reported, and silver oxides doped with other metals are receiving increased interest for their stability and electrical properties [7, 8]. Microstructured AgO deposited by electrodeposition has been demonstrated to be a useful material for surface-enhanced Raman spectroscopy [9].

$AgCuO_2$ is thought to have a low direct band gap, estimated to be 0.2–0.7 eV [10], making it a candidate solar absorber, although recent experiments on single crystals suggest that the material may be a quasi-metal with delocalized charges [11]. Preparation of the material is still challenging. Several approaches for producing copper silver oxides have been used. $AgCuO_2$ powder can be made by mixing nitrates in a high pH solution, using K_2SO_8 as an oxidant [12–14], and hydrothermal synthesis results in crystalline particles up to 1 μm across [11]. As pointed out by Curda [13], AgO and CuO have strikingly different properties, and in $AgCuO_2$, the valence of the silver and copper is different. It is therefore interesting to explore the stability of one phase (e.g., AgO) under additions of the other metal, e.g., copper. RF sputtering resulted in thin film deposits of a mixture of $AgCuO_2$ and $Ag_2Cu_2O_3$ [15] or pure $AgCuO_2$ [16, 17]. Pure $Ag_2Cu_2O_4$ powder has been produced by electroreduction, using 0.46 V versus a Pt wire quasi-reference in a solution containing $Ag_2Cu_2O_3$ and NaOH [18].

In this work, we report the use of nitrates as source materials for electrodeposition of this family of materials. This resulted in deposition of thin films of mixed oxides and microparticles of single-phase copper-doped AgO.

Experimental

Deposition

Substrates used were n-type silicon (resistivity 10–100 Ω cm) or PtSi (~50 nm) on silicon. Prior to deposition, substrates were sonicated in isopropanol and blown dry with compressed nitrogen gas. All samples were prepared at room temperature.

A. M. Fyhn · X. Yang · M. Nematollahi · J. C. Walmsley · U. J. Gibson (✉)
Department of Physics, Norwegian University of Science and Technology, 7491 Trondheim, Norway
e-mail: ursula.gibson@ntnu.no

J. C. Walmsley
SINTEF, Materials and Chemistry, 7491 Trondheim, Norway

Control samples of copper and silver oxides were prepared from the individual nitrates; these solutions were titrated to the pH values indicated in Table 1.

AgO has a band gap of 1.1 eV and has been electrodeposited by Breyfogle et al. [19]. In their process, a silver acetate solution mixed with sodium acetate was used as test solution, while a silver wire acted as reference electrode. Metallic silver deposition occurred at −0.07 V versus this reference, and silver oxide was deposited at positive voltages (current density 0.25 mA/cm^2). Silver oxide deposition followed the reactions below when in an alkaline solution [20], where potentials are referenced to a normal hydrogen electrode as follows:

$$2Ag(s) + 2OH^- \rightarrow Ag_2O + H_2O + 2e^-; E_0 = 0.34\ V \quad (1)$$

$$Ag_2O(s) + 2OH^- \rightarrow Ag_2O_2 + H_2O + 2e^-; E_0 = 0.6\ V \quad (2)$$

For the deposition of $Ag_{1-x}Cu_xO$, a solution of mixed copper and silver nitrates was prepared at a concentration of 2.5 mM for each nitrate. To the mixed nitrate, we added a variable volume of 50 mM NaOH, resulting in the concentrations given in Table 1 and an initial pH of 10–12, depending on the addition. The pH dropped during subsequent reaction of the hydroxides and nitrates. At 25 mM NaOH, a light green solution was initially observed from which dark precipitates settled to the bottom of the beaker after approximately 30 min. Little color remained in the solution, indicating a reduction in the number of available copper ions.

Stirring was started 20 min after the NaOH addition, and the substrate was placed in the solution after an additional 10 min. For the pure nitrate solutions, the solutions were titrated to the given pH values. One sample (t11b) was prepared without filtration; for this, the stirring was stopped prior to substrate insertion. A control experiment was performed using the solution remaining after removal of the precipitates with filter paper, with no deposition resulting. While the PtSi enhanced nucleation, we believe the silicide was etched in the basic solution with an anodic current, as evidenced by a high current (100 μA/cm^2) during the first minutes after application of the potential, followed by a 20-fold reduction to the steady-state deposition level.

Table 1 Deposition Conditions

Sample ID	NaOH (mM)	Time (h)	Substrate	V_0(V)
t10	25	24	PtSi	0.9
t11b	10	24	Si	0.9
t12	25	72	Si	0.9
t14	25	72	Si	1.2
t15	25	72	Si	0.0
AgO	pH 12	24	Si	0.9
CuO	pH 11	24	Si	0.9

The conditions and applied voltages for the samples are as shown in Table 1. Depositions were made from mixed nitrates as well as solutions that contained each nitrate separately. In early depositions, precipitate particles were observed to be electrostatically attracted to the substrates, so a double layer of nylon mesh (hole size 0.1 mm) was placed around the substrate in later runs to prevent particulate attachment.

Samples were deposited under the control of a Pine Instruments WaveNow Potientiostat. To avoid contamination, a silver counter-electrode was used in a two-electrode configuration. The substrate was biased at 0, 0.9, or 1.2 V relative to the silver. We did not use a reference electrode, as we found that there was contamination of the films using either an Ag/AgCl electrode or a salt bridge. Current densities during deposition were 5–10 μA/cm^2.

Analysis

Analysis of the films was made by x-ray diffraction (XRD), scanning electron microscopy (SEM), energy dispersive x-ray spectroscopy (EDS), and Auger analysis. SEM images and EDS analysis were obtained on a Zeiss Ultra 55 instrument with a Bruker EDS spectrometer operating at 5 kV. X-ray diffraction studies were performed using a Bruker D8 Focus. Auger analysis was performed on a JEOL 9500F at 10 kV.

Results and discussion

Morphology

Deposition from a stirred solution containing precipitates (determined by XRD to be $Ag_2Cu_2O_3$) resulted in a continuous film of mixed oxide phases. All of the filtered runs resulted in deposits with incomplete substrate coverage.

To provide a baseline, depositions were made with each of the nitrates separately. Figure 1a, b show the resulting morphologies. Deposition from a solution of silver nitrate at pH 12 resulted in deposition of numerous highly ordered platelets of AgO, similar to the structure observed by Fang et al., but with better-developed crystal facets [9]. An attempt to grow copper oxide from a nitrate solution at pH 12 resulted in no deposition, as all copper precipitated out at this pH. The pH was reduced to 11 for the deposition shown.

Figure 2 shows the growth habit of material deposited onto silicon from mixed nitrates at 25 mM NaOH with an applied voltage of 0.9 V (sample t12), which exhibits three-dimensional growth as well as well-defined platelets. When the deposition solution was filtered, growth was slow, but large crystals of $Ag_{1-x}Cu_xO$ resulted. All high-magnification images revealed reduced quality in the platelet material grown

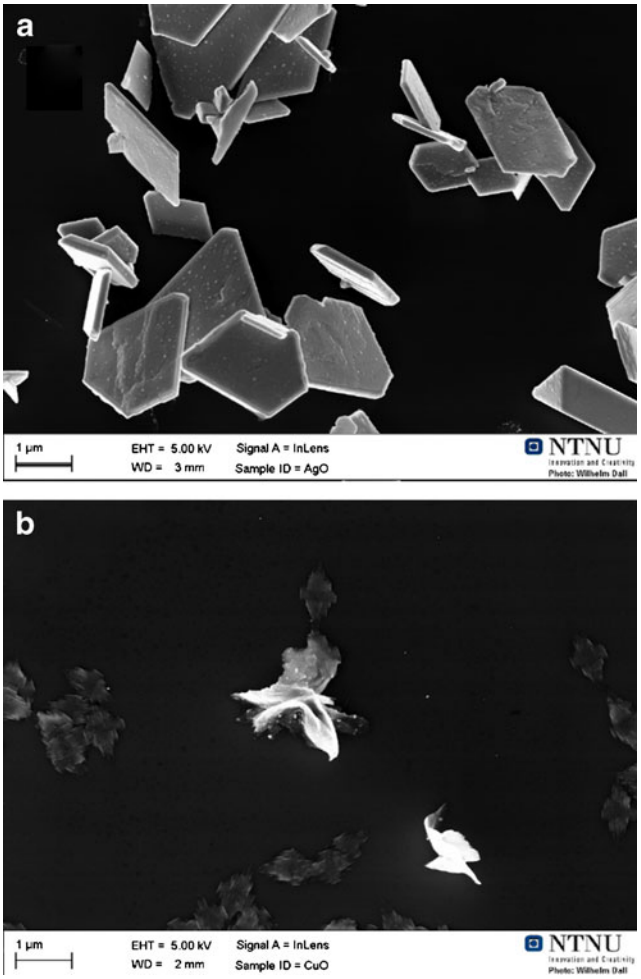

Fig. 1 Deposition from individual nitrates. **a** Platelets of AgO and **b** clumps of copper oxides/hydroxides. *Scale bars* are 1 µm

from mixed nitrates, which is reflected in the x-ray diffraction results (see below). Chemical analysis did not indicate a difference in the composition of the two- and three-dimensional grains. Deposition at 10 mM NaOH reduced the nucleation barrier and resulted in aggregates of two-dimensional nanoparticles, as shown in Fig. 3. Concentrations of NaOH below 10 mM resulted in co-deposition of metallic silver.

Figure 4 shows the morphology resulting from variation of the voltage for depositions on n-type silicon. With 25 mM NaOH and no applied voltage, randomly deposited small clumps and crystals were seen, while at 0.9 V, large oriented crystals were observed, similar to AgO platelets, but with more three-dimensional character and apparent disorder due to the inclusion of copper. At 1.2 V, increased nucleation was seen, with mixture of morphologies and overall reduction in crystal size.

X-ray diffraction

XRD results for the films (color online) are show in Fig. 5, and data on the major diffraction peaks of related materials are shown in Table 2. All scans were referenced to the Si peak at 32.96°, which may either be the forbidden (200) $K\alpha_1$ peak from multiple scattering [21], or (211) reflections from small silicon particles on the surface, to correct for any sample height variation during data acquisition. For our samples, peak positions were determined using a peak-fitting routine in MATLAB to separate the overlapping peaks in the vicinity of 32°. Peaks were scaled and offset to improve visibility. X-ray diffraction on samples deposited from the silver nitrate solution gave a large signal at 32.03° associated with the AgO (200) reflection, but the intensity of the reflections at 32.3 and 34.16° were smaller than for the powder files. The two-dimensional growth habit of the crystals, rather than strongly oriented growth, is thought to be responsible for the emphasis of the (200) reflections at the expense of others. The broad peaks in the x-ray spectra from the copper nitrate deposition could be due to either copper oxides or $NaCuO_2$ [22].

Depositions from the mixed nitrates with 25 mM NaOH and an applied substrate voltage of 0.9 V showed peaks at similar positions, but with slightly larger angles and with the

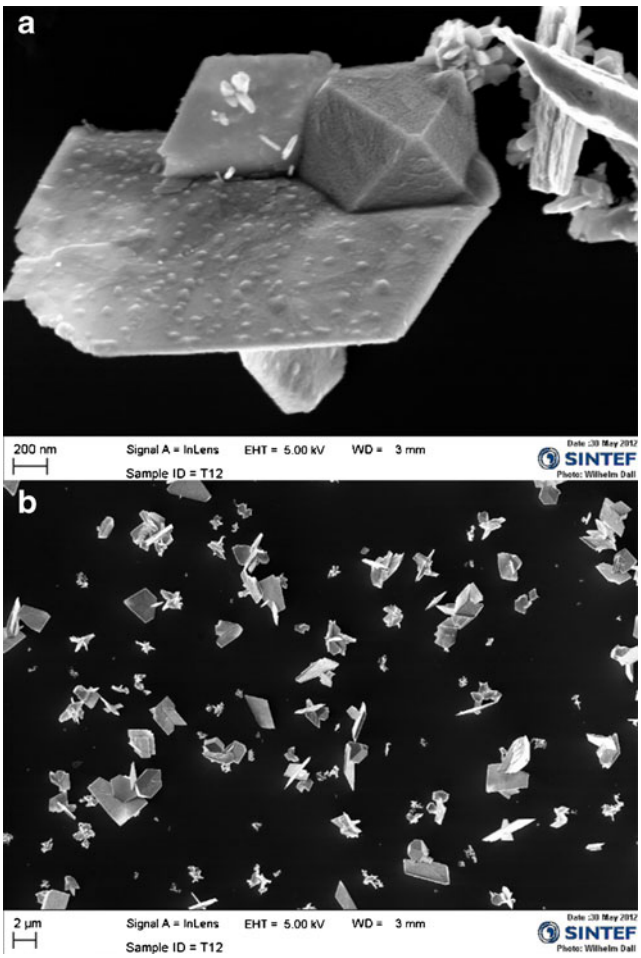

Fig. 2 Sample t12, deposited with 25 mM NaOH at 0.9 V **a** detail and **b** overview. Small deposits (bumps) are residual NaOH. *Scale bars* are 200 nm and 2 µm

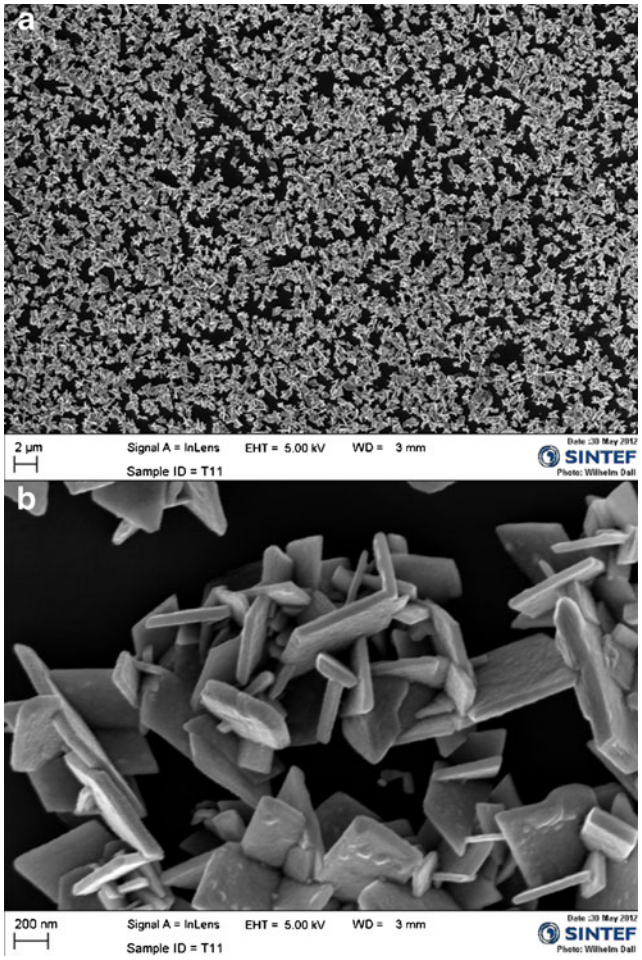

Fig. 3 Sample t11b, deposited with 10 mM NaOH at 0.9 V **a** overview and **b** detail. *Scale bars* are 2 µm and 200 nm

intensity spread more evenly among the lines. The peak shift suggests inclusion of copper in the lattice, given the smaller radius of copper ions. We have not found literature results on substitutional copper in silver oxides, but the silver oxides are known to have a mixture of Ag(I) and Ag(III), substitution at the former sites, as Cu(I) seems most probable. It was not possible to determine the valence state of the Cu directly from the Auger results, but XPS studies in the future may confirm this hypothesis. The x-ray intensity redistribution correlates with our observation of the presence of both two- and three-dimensional crystals. While we cannot rule out the existence of more than one phase, Auger and EDS analyses showed comparable amounts of copper in all the individual crystals examined. The relative heights of the doublet peaks near 32° was a strong function of copper inclusion, and the peaks shifted to higher angle for the deposition of material deposited with 10 mM NaOH, where there was more available copper. Silicon peaks, not visible in scans of the PtSi-coated substrate, are visible through the deposited film. These small peaks may arise due to the nonuniform thickness of the film, or possibly from post-deposition scratches. The film consists of a uniform layer estimated to be 5–10 nm thick, with three-dimensional structures up to 400 nm in size on top of the continuous layer.

The sample deposited at 1.2 V and 25 mM NaOH is closer in structure to the pure AgO film than those deposited at lower voltages. This may result from a change in the local pH at the surface of the substrate, which reduces incorporation of copper from the growth solution.

Chemical analysis

Spot analysis was performed with both EDS in a scanning electron microscope and Auger electron spectroscopy on several of the crystals from the mixed nitrate depositions. Both measurements clearly showed the incorporation of copper, with an approximate composition of 2–3 % copper by both techniques. Figure 6 shows the Auger signal for t12, deposited at 0.9 V, which has small deposits on the crystal faces. Other spectra showed no evidence of sodium inclusion. Four different crystals, some flat, and some three-dimensional were analyzed using quantitation software, but did not reveal statistically significant differences in the copper concentration. The sodium peak is thought to arise from incomplete rinsing of NaOH after deposition. EDS results (not shown) for samples deposited with 25 mM NaOH at 0.9 V yielded a ratio of copper to silver between 2.5 and 3 %. Multiple crystals were

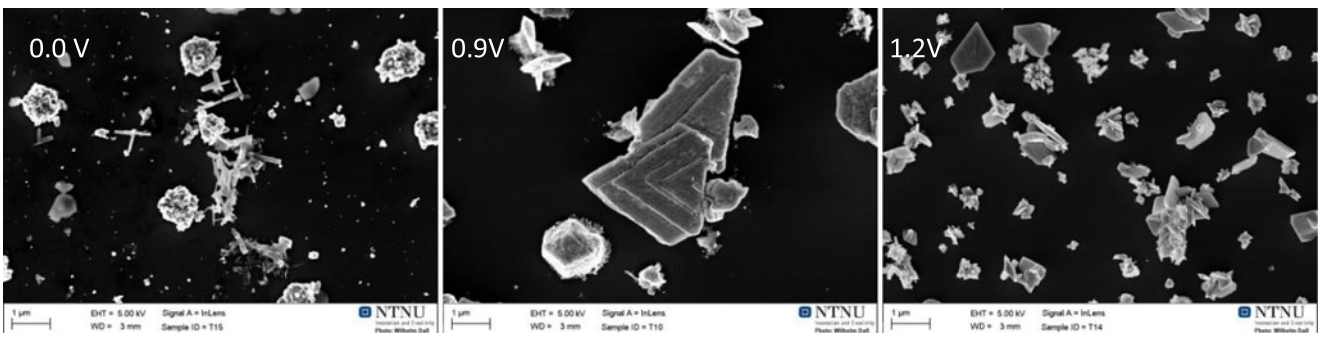

Fig. 4 Samples deposited at 0, 0.9, and 1.2 applied volts using 25 mM NaOH. *Scale bars* are 1 µm

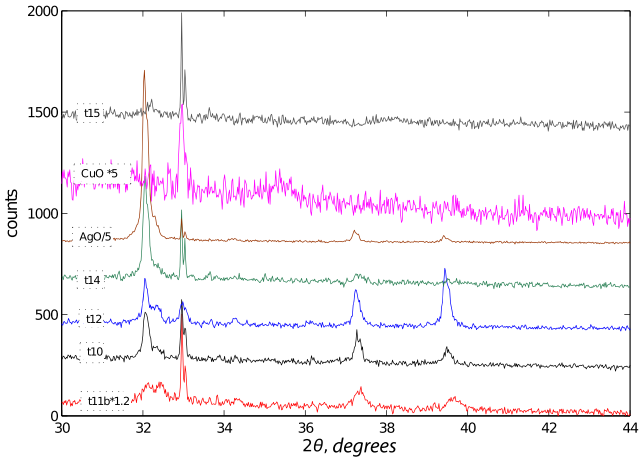

Fig. 5 X-ray diffraction results for films deposited at different pH and applied voltage. (Color online) Peak amplitudes (as indicated) and baselines have been adjusted to improve readability

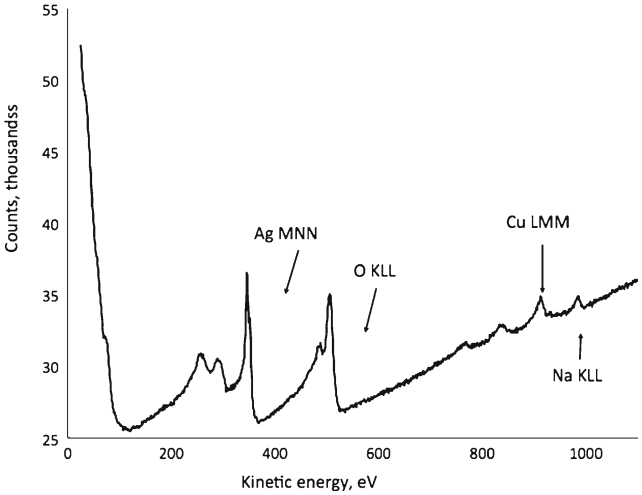

Fig. 6 Auger survey scan for a particle on sample t10, dominated by oxygen, silver, and copper peaks

examined and gave similar results; no additional peaks were observed except for those from the silicon substrate.

Discussion and conclusions

Although deposition of copper oxides is typically performed cathodically, we find that small amounts of copper can be incorporated into silver oxide nanocrystals during anodic deposition. The copper ions for this reaction are liberated from the $Ag_2Cu_2O_3$ precipitate which forms when the silver and copper nitrates react with NaOH. There is a limited range of hydroxide concentrations that results in the deposition of these materials; if there is too little, films with metallic silver are formed, whereas too high, a concentration drives the equilibrium between the precipitate and the solution so far toward the solid that no copper is available for deposition. Likewise, only a narrow range of applied voltages results in the growth of ordered crystals. At low applied voltages, the only particles on the substrate are those that adventitiously deposit despite the filter. The appearance of large ordered nanoparticles in the presence of an applied voltage demonstrates that these are growing via an electrodeposition process. If the voltage is increased beyond 1.0 V, the quality of the deposit degrades; although growth of small particles is observed, the reduced nucleation barrier results in more numerous smaller crystals. The x-ray signature for these samples is similar to that of the films deposited in the absence of copper. This may be due to a reduced effective pH in the vicinity of the substrate. This is not uniform across the substrate due to the resistance of the silicon, and may be expected to extract copper preferentially near the electrolyte surface.

Additional work to determine the optical properties will clarify the role of the copper in the silver, but in this work, with low coverage on silicon substrates, reliable optical measurements were not possible. Techniques to lower the nucleation barrier, such as pre-coating the substrate with a suitable

Table 2 ICDD data (bold column headings) release 1/2012, for selected silver copper oxides, along with peak positions for two samples. The first value is the peak position, and the second is relative intensity

AgO[a]	$AgCuO_2$[b]	Ag_2O[c]	CuO[d]	AgO	t11b
32.0064–50	30.9376–897		32.4788–73	32.03	32.1
32.2793–100	32.0816–623	33.9282–4	35.3844–313	32.3	32.4
34.1683–35	35.5371–207		35.5384–783	34.2	34.34
37.1837–86	37.1899–764	36.4949–4	38.6389–999		
39.383–36	39.3087–104	38.6095–100	38.9688–221	39.44	39.64
	41.1788–999				

[a] PDF 00-043-1038

[b] PDF 04-009-8251

[c] PDF 00-019-1155

[d] PDF 04-005-4712

metal, may be useful in this regard. The apparent change in the lattice constant makes it likely that there will be an associated change in the band gap.

We have demonstrated one-step room temperature electrodeposition of $Ag_{1-x}Cu_xO$ from a solution of mixed nitrates at high pH. The material deposits as individual nanoparticles, demonstrating a high barrier to nucleation on silicon substrates. Incorporation of copper into the lattice increases the lattice spacing, and the widths of the peaks in x-ray diffraction suggest that there are substantial defect densities within the crystallites. Auger and EDX analysis indicates incorporation of ~3 % copper into the lattice.

References

1. Golden TD, Shumsky MG, Zhou YC, VanderWerf RA, VanLeeuwen RA, Switzer JA (1996) Chem Mater 8:2499–2504
2. Septina W, Ikeda S, Khan MA, Hirai T, Harada T, Matsumura M, Peter LM (2011) Electrochim Acta 56:48824888
3. Fortin E, Masson D (1982) Solid-State Electronics 25:281283
4. Katayama J, Ito K, Matsuoka M, Tamaki J (2004) J of Appl Electrochem 34:687692
5. Jeong SS, Mittiga A, Salza E, Masci A, Passerini S (2008) Electrochim Acta 53:22262231
6. Ida Y, Watase S, Shinagawa T, Watanabe M, Chigane M, Inaba M, Tasaka A, Izaki M (2008) Chem Mater 20:1254–1256
7. Subrahmanyam A, Barik UK (2007) J Mater Sci 42:6041–6045
8. Shima T, Buechel D, Mihalcea C, Kim J, Atoda N, Tominaga J (2003) Top in Appl Phys 88:49–58
9. Fang C, Ellis AV, Voelcker NH (2012) Electrochim Acta 59:346–353
10. Feng J, Xiao B, Chen JC, Zhou CT, Du YP, Zhou R (2009) Solid State Commun 149:1569–1573
11. Muñoz-Rojas D, Córdoba R, Fernández-Pacheco A (2010) María De Teresa J, Sauthier G, Fraxedas J, Walton RI, Casañ-Pastor N. Inorg Chem 49:10977–10983
12. Gomez-Romero P, Tejada-Rosales E, Palacin MR (1999) Angew Chem Int Ed Engl 38:524
13. Curda J, Klein W, Jansen M (2001) J of Solid State Chem 162:220–224
14. Curda J, Klein W, Liu H, Jansen M (2002) J of Alloys Compd 338:99103
15. Pierson JF et al (2006) Appl Surf Sci 253:1484–1488
16. Lund E, Galeckas A, Monakhov E, Svensson BG (2011) Thin Solid Films. doi:10.1016/j.tsf.2011.07.030
17. Lund E, Galeckas A, Monakhov EV, Svensson BG (2012) Phys Stat Solidi C9:1590–1592
18. Munoz-Rojas D, Oró J, Gómez-Romero P, Fraxedas J, Casañ-Pastor N (2002) Electrochem Commun 4:684–689
19. Breyfogle BE, Hung CJ, Shumsky MG, Switzer JA (1996) J Electrochem Soc 143:2741–2746
20. Aylward G , Findlay T, SI chemical data 5th ed, 2002, John Wiley & Sons Australia Ltd, ISBN-13 978 0 470 800444 7
21. Tischler JZ, Budai JD, Ice G, Habenschuss J (1988) Acta Cryst A44:22–25
22. Pickardt J, Paulus W, Schmalz M, Schöllhorn R (1990) J Sol State Chem 89:308